[2]Lijewski, L. E., and Suhs, N., "Time-Accurate Computational Fluid Dynamics Approach to Transonic Store Separation Trajectory Prediction," *Journal of Aircraft*, Vol. 31, No. 4, 1994, pp. 886–891.

[3]Hall, L. H., Mitchell, C. R., and Parthasarathy, V., "An Unsteady Simulation Technique for Missile Guidance and Control Applications," AIAA Paper 97-0636, Jan. 1997.

[4]Schindel, L. H., "Store Separation," AGARD-AG-202, June 1975.

[5]Arnold, R. J., and Epstein, C. S., "Store Separation Flight Testing," AGARD Flight Test Techniques Series, edited by R. K. Bogue, AGARD-AG-300, Vol. 5, Arnold Engineering Development Center, Arnold AFB, TN, April 1986, pp. 14–16.

[6]Heim, E., "CFD Wing/Pylon/Finned-Store Mutual Interference Wind Tunnel Experiment," Arnold Engineering Development Center AEDC-TSR-91-P4, Arnold AFB, TN, Jan. 1991.

[7]Jordon, J. K., "Computational Investigation of Predicted Store Loads in Mutual Interference Flow Fields," AIAA Paper 92-4570, Aug. 1992.

[8]Kiber, G. M., "An Analysis to Determine the Amount of Wind Tunnel Grid Data Required to Provide Acceptable Trajectory Simulation Accuracy at Minimum Cost," ARO Inc., Arnold Engineering Development Center, AEDC-TMR-80-G41, Arnold AFB, TN, Dec. 1980.

[9]Strash, D. J., and Tidd, D. M., "MGAERO—Users' Manual," Analytical Methods, Inc., Redmond, WA, June 1998.

[10]Vukelich, S. R., Stoy, S. L., and Bruns, K. A., "Missile Datcom. Vol. I—Final Report," Air Force Flight Dynamics Lab., AFWAL-TR-86-3091, Dec. 1988.

[11]"Simulink User's Guide," The MathWorks, Inc., Ver. 1.3, Natick, MA, 1993.

Prediction of Vortex Breakdown Location on a Banked Delta Wing

Alain Pelletier* and Robert C. Nelson†
University of Notre Dame, Notre Dame, Indiana 46556

Introduction

AN experimental study of leading-edge vortex breakdown on a family of delta wings was conducted at the University of Notre Dame.[1,2] Flow visualization and image processing techniques were used to measure the location of vortex breakdown as a function of static angle of attack and roll angle.

Measurement of the location of vortex breakdown on slender flat-plate delta wings has been obtained by numerous investigators.[3–5] These studies examined breakdown on simple delta wing models for static conditions. Over the years, researchers have tried to determine what factors influence breakdown. Elle[6] showed that the sweep angle of the wing significantly affects breakdown. He found that increasing the sweep angle moves vortex breakdown downstream for a given angle of attack. Kegelman and Roos[5] presented results that showed that breakdown is influenced by the leading-edge geometry of the wing. The trailing-edge geometry might also have some influence on the location of vortex breakdown because it might affect the adverse pressure gradient at the trailing edge. O'Neil et al.[7] showed that the adverse pressure gradient is imposed by the trailing edge and that it has an effect on breakdown location. The sideslip angle is another parameter that influences breakdown.

In the present investigation, an attempt was made to approximate the static vortex breakdown location of a rolling 65-deg delta wing from vortex breakdown results in pitch for several wings of different sweep angles.

Received 10 May 1999; revision received 28 March 2000; accepted for publication 3 April 2000.

*Postdoctoral Research Assistant, Department of Aerospace and Mechanical Engineering. Member AIAA.

†Professor, Department of Aerospace and Mechanical Engineering. Fellow AIAA.

Table 1 Delta wings

Sweep angle, deg	Chord, in. (cm)	Span, trailing edge, in. (cm)
50	8 (20.32)	13.43 (34.11)
55	8 (20.32)	11.20 (20.45)
60	8 (20.32)	9.24 (23.47)
65	14 (35.56)	13.06 (33.16)
70	14 (35.56)	10.2(25.91)
75	14 (35.56)	7.5 (19.05)
80	14 (35.56)	4.9 (12.45)

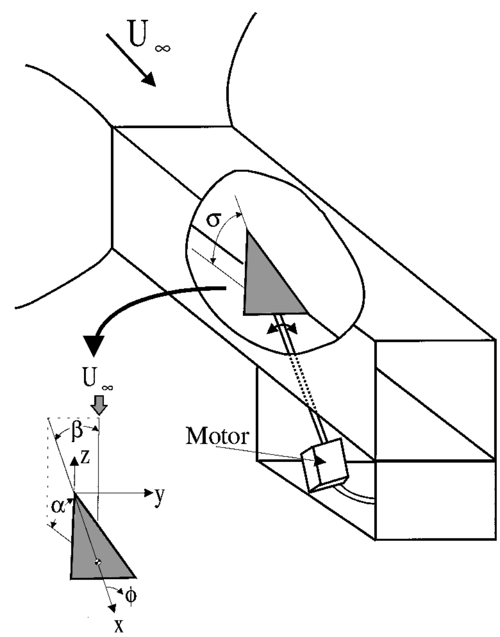

Fig. 1 Test section arrangement for rolling tests.

Apparatus

A family of flat-plate delta wings with sweep angles varying from 50 to 80 deg were built for this research program. Table 1 shows the dimensions of the wings as a function of sweep angle. All of the wings had a thickness of 0.25 in. (6.4 mm), a 45-deg bevel on the bottom surface and a blunt trailing edge. This Note will focus on the results for a 65-deg delta wing at a root-chord Reynolds number, $Re = 1 \times 10^5$.

All experiments were performed in a 2×2 ft (0.609×0.6096 m) indraft subsonic wind tunnel at the University of Notre Dame. Each wing was tested for different static angles of attack (no roll) and for different roll angles (for a fixed sting angle of attack σ). Figure 1 shows a schematic of the delta wing arrangement in the wind tunnel for the rolling experiments. For the experiments in pitch, a U-shaped pitching yoke was used.[1,8]

All tests were directed toward measuring vortex breakdown location as a function of the angle of attack and roll angle. For the flow visualization, titanium tetrachloride ($TiCl_4$) was injected into the flow near the apex of the wings. The dense white smoke generated by the reaction between the $TiCl_4$ and air moisture was entrained by the vortices over the wings, and breakdown could easily be observed.[9] A charge-coupled device video camera in super video home system mode was used to record the flow visualization data. Image processing equipment and software were used to analyze the flow images and to obtain measurements of the vortex breakdown location.

Results

Pitch Tests

Static pitching tests on the series of delta wings at $Re = 1 \times 10^5$ gave the results presented in Fig. 2. As was expected, vortex breakdown moved upstream (toward the apex at $x/c = 0$) with increasing angle of attack. Moreover, increasing the sweep angle

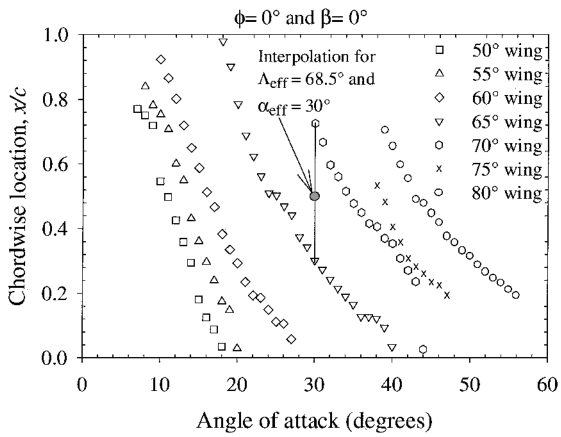

Fig. 2 Chordwise location of vortex breakdown in static pitch for several wings; uncertainty in α = ± 0.3 deg and uncertainty in x/c = 5%.

delayed vortex breakdown. The locations of vortex breakdown presented in Fig. 2 are the average of the left and right vortex breakdown locations for 10 video frames (a total of 20 readings). The breakdown location varied from one frame to another due to the unsteady nature of vortex breakdown. Moreover, it was assumed that breakdown was perfectly symmetric, which was not always the case with the oscillations. These small differences in breakdown location on both sides of the wing from one frame to another introduced an uncertainty in the exact breakdown location. It was determined that this led to an uncertainty of approximately 5%.

Roll Tests

It is known that rolling a delta wing about its longitudinal axis (mounted at incidence angle of attack σ) creates an effective sideslip angle and an effective angle of attack. The effective sideslip modifies the effective sweep angle of both sides of the wing. For the side of the wing rolling upward (leeward side), the effective sweep increases. It decreases on the side of the wing rolling downward (windward side). Equations (1) and (2) show how the angle of attack α and the sideslip angle β vary with roll:

$$\alpha(\phi) = \tan^{-1}(\tan\sigma\cos\phi) \quad (1)$$

$$\beta(\phi) = \tan^{-1}(\tan\sigma\sin\phi) \quad (2)$$

For the effective sweep angle, we assume, as in Ref. 10

$$\Lambda_{\text{eff}}(\phi) = \Lambda_0 \pm \beta(\phi) \quad (3)$$

with $+$: port side of the wing and $-$: starboard side of the wing and where Λ_0 is the sweep angle of the wing.

Vortex breakdown location results were obtained for the 65-deg delta wing at a sting angle $\sigma = 30$ deg. The sting angle corresponds to the angle of attack of the wing for $\phi = 0$ deg. The experiments were conducted at a Reynolds number of 1×10^5. Vortex breakdown location at static roll angles for the 65-deg delta wing is presented in Fig. 3. As the wing rolls, breakdown on the leeward side of the wing propagates downstream toward the trailing edge ($x/c = 1$), whereas breakdown on the windward side propagates upstream toward the apex. The experimental breakdown locations in roll presented in Fig. 3 were once again obtained by averaging 10 video frames. In this case, however, the left and right breakdown locations were not averaged together because breakdown is not symmetric in roll.

Interpolation of the data presented in Fig. 2 was performed to approximate the experimental roll data of Fig. 3. For the interpolations, one first interpolates for x/c at the effective angle of attack on curves of constant Λ. Then, a linear interpolation between the two curves of constant Λ for the effective sweep angle leads to the interpolated x/c for a given roll angle. An example of the interpolation in Λ is shown in Fig. 2 for an effective sweep angle of 68.5 deg and an effective angle of attack of 30 deg. As is also presented in Fig. 3, the interpolated data indicate the same trends as the

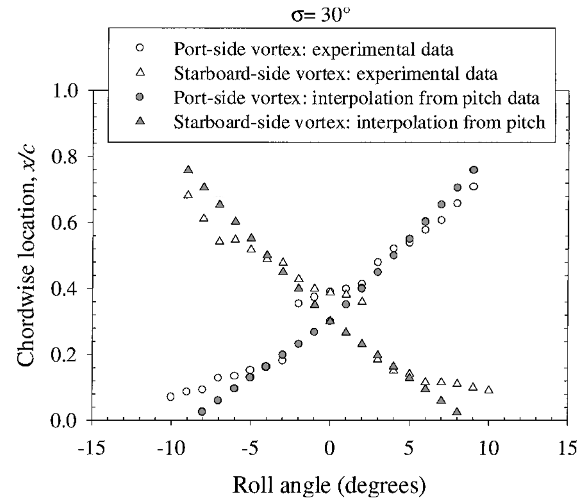

Fig. 3 Static roll vortex breakdown location for a 65-deg delta wing; uncertainty in α = ± 0.3 deg and uncertainty in x/c = 5%.

experimental roll data. Moreover, there seems to be a good agreement between the two sets of data, except around $\phi = 0$ deg (from -2 to 2 deg). The discrepancy is believed to be caused by sting interference. At large roll angles, the windward vortex is closer to the sting than the leeward vortex. The effect of an adverse pressure gradient due to the sting would be to promote breakdown on the windward side (farther upstream). As the roll angle is decreased, the distance between the windward vortex and the sting increases. At some point, close to $|\phi| = 2$ deg, the adverse effect of the sting is reduced, and the vortex breakdown is less affected by the sting and moves downstream quickly. Ericsson and Beyers[11] have reviewed the issue of sting interference and their paper can be consulted for further information.

Conclusions

Static vortex breakdown results seem to indicate that vortex breakdown location data in static pitch can be used to approximate the vortex breakdown location on a statically rolled 65-deg delta wing. This tends to show that, within the range of parameters investigated, vortex breakdown is a function of effective sweep angle and effective angle of attack.

Acknowledgments

This project was sponsored by the Institute for Aerospace Research Canada. The authors wish to thank Ernest Hanff for assistance during this study.

References

[1] Pelletier, A., "An Experimental Investigation of Vortex Breakdown on Slender Delta-Wing Planforms," Master's Thesis, Dept. of Aerospace and Mechanical Engineering, Univ. of Notre Dame, Notre Dame, IN, April 1994.

[2] Pelletier, A., and Nelson, R. C., "An Experimental Study of Static and Dynamic Vortex Breakdown on Slender Delta-Wing Planforms," AIAA Paper 94-1879, June 1994.

[3] Wentz, W. H., and Kohlman, D. L., "Vortex Breakdown on Slender Sharp-Edged Wings," *Journal of Aircraft*, Vol. 8, No. 3, 1971, pp. 156–161.

[4] Erickson, G. E., "Flow Studies of Slender Wing Vortices," AIAA Paper 80-1423, 1980.

[5] Kegelman, J. T., and Roos, F. W., "Effects of Leading-Edge Shape and Vortex Burst on the Flowfield of a 70-Degree-Sweep Delta Wing," AIAA Paper 89-0086, Jan. 1989.

[6] Elle, B. J., "An Investigation at Low Speed of the Flow Near the Apex of Thin Delta Wings with Sharp Leading Edges," Aeronautical Research Council, R&M 3176, British Aeronautical Research Council, Jan. 1958.

[7] O'Neil, P. J., Roos, F. W., Kegelman, J. T., Barnett, R. M., and Hawk, J. D., "Investigation of Flow Characteristics of a Developed Vortex," Naval Air Development Center, McDonnell Aircraft Co., St Louis, MO, Rept. NADC-89114-60, 1989.

[8] Grismer, D. S., and Nelson, R. C., "Double-Delta-Wing Aerodynamics for Pitching Motions With and Without Sideslip," *Journal of Aircraft*, Vol. 32, No. 6, 1995, pp. 1303–1311.

[9]Visser, K. D., Nelson, R. C., and Ng, T. T., "Method of Cold Smoke Generation for Vortex Core Tagging," *Journal of Aircraft*, Vol. 25, No. 11, 1988, pp. 1069–1071.

[10]Huang, X. Z., and Hanff, E. S., "Prediction of Leading-Edge Vortex Breakdown on a Delta Wing Oscillating in Roll," AIAA Paper 92-2677, June 1992.

[11]Ericsson, L. E., and Beyers, M. E., "Ground Facility Interference Effects on Slender Vehicle Dynamics," AIAA Paper 95-0795, 1995.

Application of Finite Strip Method to Composite Panel Flutter Analysis

L. C. Shiau* and S. T. Hwang†
National Cheng-Kung University, Tainan 70101, Taiwan, Republic of China

Introduction

COMPOSITE materials have been widely used in aeronautical industries to replace metals in the aircraft structures for the purpose of weight saving. Currently, in high-performance aircraft, composite materials are mostly used to make the skins of wings and fuselage of an aircraft. During high-speed flight, the external skin panel of an airframe may exhibit flutter. This type of aeroelastic instability has received much attention in the past 40 years.[1,2] Because the finite-element method (FEM) was first applied to panel flutter by Olson[3] in 1967, it has gained widespread attention by aeroelasticians, and many panel flutter analyses were done by using the FEM.[4,5] Although the FEM is the most powerful and versatile tool of solution in panel flutter analysis, it may be unnecessary for structures that have regular geometric plans and simple boundary conditions. Hence an alternative method that can reduce the computational effort, but at the same time, retain to some extent, the versatility of the finite-element analysis, is desirable. In this Note, the finite-strip method (FSM) developed by Cheung[6] in 1968 is applied to the flutter analysis of composite panels.

Equation Formulation

Consider a symmetric composite laminated thin plate with length a, width b, thickness h, and mass density per unit volume ρ, as shown in Fig. 1. The plate is assumed to consist of N layers of homogeneous anisotropic sheets bonded together. Supersonic airflow with air density ρ_a, flow velocity U_a, Mach number M_∞, and aerodynamic pressure Δp is assumed passing over the top surface of the plate with an angle Λ measured counterclockwise from the x axis.

The governing differential equation of motion for the plate can be obtained as

$$D_{11}\frac{\partial^4 w}{\partial x^4} + 4D_{16}\frac{\partial^4 w}{\partial x^3 \partial y} + 2(D_{12} + 2D_{66})\frac{\partial^4 w}{\partial x^2 \partial y^2} + 4D_{26}\frac{\partial^4 w}{\partial x \partial y^3} + D_{22}\frac{\partial^4 w}{\partial y^4} + \rho h\frac{\partial^2 w}{\partial t^2} + \Delta p = 0 \tag{1}$$

where w is the normal displacement of the plate. The flexural and torsional rigidities D_{ij} of the plate take the form of

$$D_{ij} = \frac{1}{3}\sum_{k=1}^{N}(\bar{Q}_{ij})_k\left(z_k^3 - z_{k-1}^3\right), \qquad (i, j = 1, 2, 6) \tag{2}$$

Received 17 October 1999; revision received 10 January 2000; accepted for publication 20 March 2000.

*Professor, Institute of Aeronautics and Astronautics; lcs@mail.iaa.ncku.edu.tw.

†Former Graduate Student, Institute of Aeronautics and Astronautics.

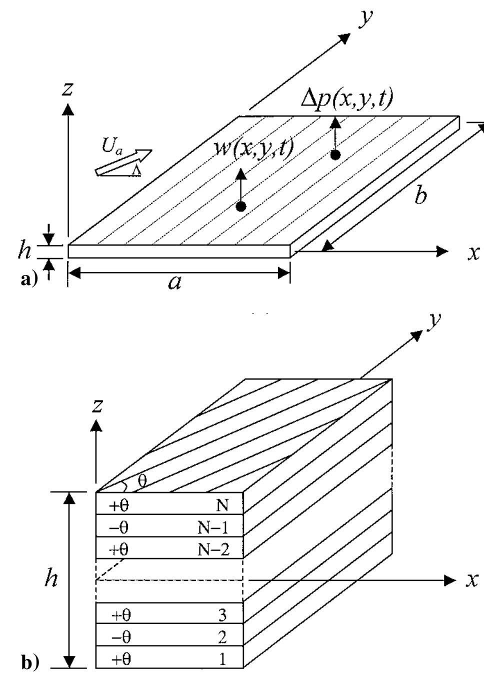

Fig. 1 a) Panel geometry and mesh divisions, and b) ply-stacking sequence.

where $(\bar{Q}_{ij})_k$ is the transformed reduced stiffness of the kth layer and z_k is defined in Fig. 1. The aerodynamic pressure Δp is approximated by quasi-steady aerodynamic theory as

$$\Delta p(x, y, t) = \frac{-\rho_a U_a^2}{(M_\infty - 1)^{\frac{1}{2}}}\left(\frac{\partial w}{\partial x}\cos\Lambda + \frac{\partial w}{\partial y}\sin\Lambda + \frac{1}{U_a}\frac{M_\infty^2 - 2}{M_\infty^2 - 1}\frac{\partial w}{\partial t}\right) \tag{3}$$

When the FSM is used for the analysis, the plate is divided into several strips, as shown in Fig. 1. The displacement function $w(x, y)$ for a strip is assumed as

$$w(x, y) = \sum_{m=1}^{r} f_m(x)Y_m(y) \tag{4}$$

where $f_m(x)$ is a polynomial function in the x direction and Y_m is a series that satisfies the end conditions in the y direction. For a strip with two nodal lines and 2 degrees of freedom at each nodal line, the polynomial function is identical to that for a beam element in the FEM. The series term $Y_m(y)$ for a plate with simply supported ends is taken as

$$Y_m(y) = \sin(m\pi y/a), \qquad m = 1, 2, 3, \ldots, r \tag{5}$$

Equation (4) can also be expressed in terms of the strip nodal line displacement $\{q_s\}$ as

$$w(x, y) = \sum_{m=1}^{r} Y_m \sum_{i=1}^{4}[B_i]_m\{q_i\}_m = \sum_{m=1}^{r}[S]_m\{q_s\}_m = [S]\{q_s\} \tag{6}$$

where B_i is the shape function associated with q_i and $\{q_s\}^T = \{w_1 \;\; \theta_1 \;\; w_2 \;\; \theta_2\}$.

On substitution of Eq. (6) into Eqs. (1) and (3), the bending stiffness $[k_s]$, mass $[m_s]$, aerodynamic damping $[A_{\text{sd}}]$, and aerodynamic force $[A_{\text{sf}}]$ matrices of the strip can be obtained as

$$[k_s] = \iint [G]^T[D][G]\,\mathrm{d}x\,\mathrm{d}y \tag{7}$$

$$[m_s] = \iint \rho h[S]^T[S]\,\mathrm{d}x\,\mathrm{d}y \tag{8}$$

$$[A_{\text{sd}}] = \iint [S]^T[S]\,\mathrm{d}x\,\mathrm{d}y \tag{9}$$